Cyclotron resonance in the two-dimensional hole gas in (Ga,Al)As/GaAs heterostructures

Z. Schlesinger*
IBM Thomas J. Watson Research Center, Yorktown Heights, New York 10598

S. J. Allen, Jr.*
Bell Communications Research, Murray Hill, New Jersey 07974

Y. Yafet, A. C. Gossard, and W. Wiegmann
AT&T Bell Laboratories, Murray Hill, New Jersey 07974

(Received 25 January 1985)

Cyclotron resonance has been observed in the two-dimensional (2D) hole gas found in selectively doped heterostructures and multiple quantum wells, in magnetic fields up to 20 T. The results are compared with recent theories as well as a simple model of the 2D hole band structure obtained by taking a section through the three-dimensional valence band at a finite wave vector along the growth direction. Only rough quantitative agreement is achieved.

The orbital degeneracy at the top of the GaAs valence band[1] is expected to lead to a complex, nonparabolic set of two-dimensional (2D) bands describing holes confined to (Al,Ga)As/GaAs interfaces.[2–4] The problem of the band structure of confined holes was first addressed in earlier work on *p*-channel Si metal-oxide-semiconductor field-effect transistors[5] (MOSFET's). Here good agreement with cyclotron masses was achieved only with a self-consistent calculation of the electric subband states. Work has continued on 2D hole bands in Si MOSFET's by Wieck *et al.*[6,7] Most noteworthy is the direct observation of the lifting of the spin degeneracy of the holes by a surface electric field.

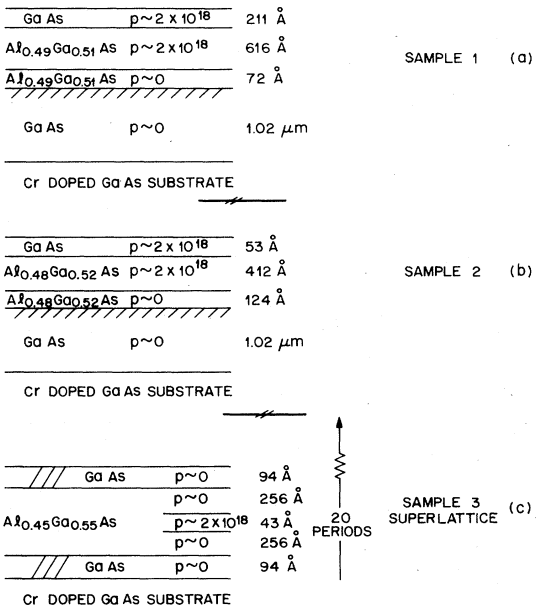

FIG. 1. The doping and layering of the samples described in the text.

The substantially higher mobilities in (Al,Ga)As/GaAs heterostructures open up the possibility of more detailed experimental studies that should reveal the rich structure expected in interband and intraband magnetoabsorption experiments[8] and provide further test of our understanding of 2D hole transport. Recently, Eisenstein *et al.*[9] have demonstrated the effect of the lifting of the spin degeneracy by surface electric fields by comparing and analyzing Shubnikov–de Haas oscillations in symmetric and asymmetric quantum wells. We report here on far-infrared cyclotron resonance (CR) experiments on the 2D hole gas in two samples with a single interface and one with multiple quantum wells. As expected, a complex spectrum emerges. We compare the results with a simple model that simulates the confinement by taking a section of the 3D band structure at a wave vector, k_z, along the growth direction, as well as more sophisticated models recently put forward.[2–4] Only rough agreement is achieved.

EXPERIMENT

The samples were prepared by molecular-beam epitaxy and are shown in Fig. 1. The single-interface samples

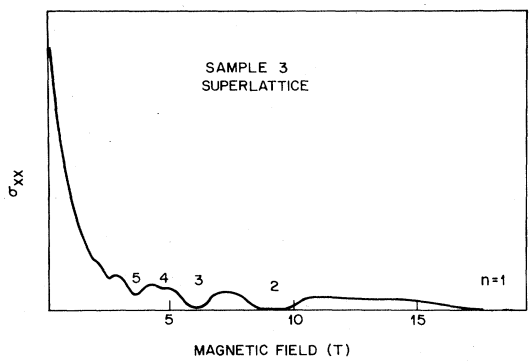

FIG. 2. Shubnikov–de Haas oscillations in σ_{xx} measured with the "pseudo-Corbino" geometry described in the text.

consist of a 1-μm undoped layer of GaAs, followed by an undoped layer of (Al,Ga)As and by a layer of (Al,Ga)As doped with Be to 2×10^{18} cm^{-3}. These samples are finally capped with a heavily doped GaAs layer which was removed before performing the transport and far-infrared measurements. In the multilayered sample a sequence of GaAs, undoped (Al,Ga)As and doped (Al,Ga)As layers were deposited. Although the background doping levels are not well known, we indicate in Table I probable signs and orders of magnitude. Table I also gives the electrical characteristics of the samples measured at 4.2 K.

Shubnikov—de Hass (SdH) oscillations in the longitudinal magnetoconductance were measured by using a "pseudo-Corbino" geometry. This consists of four or more Ohmic contacts on the perimeter of the sample and a single contact somewhere near the center. Magnetoconductance measured between the center and any one or more of the perimeter contacts yields a conductance proportional to the longitudinal conductance, σ_{xx}. The perimeter contacts can be used for measuring the sheet conductance at zero magnetic field or the Hall resistance in a field.

The SdH oscillations for the sample with multiple quantum wells, sample 3, are shown in Fig. 2. The densi-

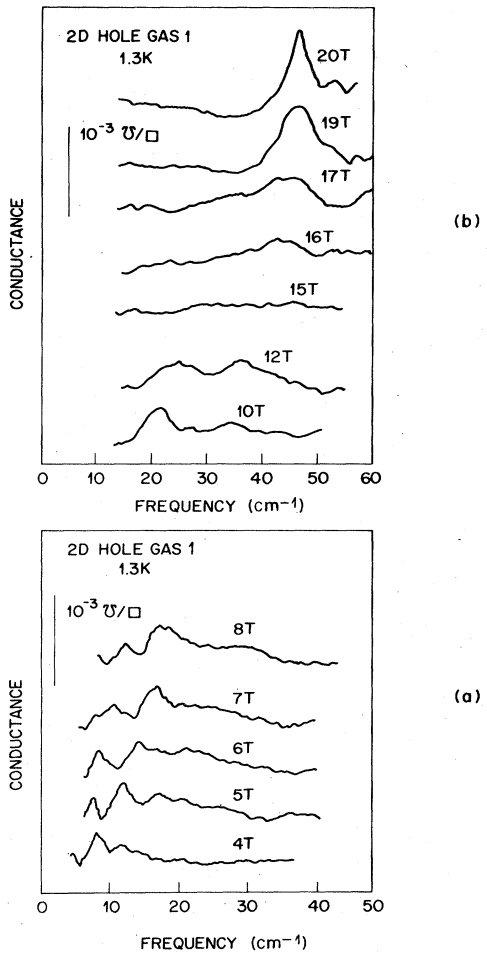

FIG. 3. Conductance versus frequency with magnetic field as a parameter at $\cong$1.3 K. Sample 1.

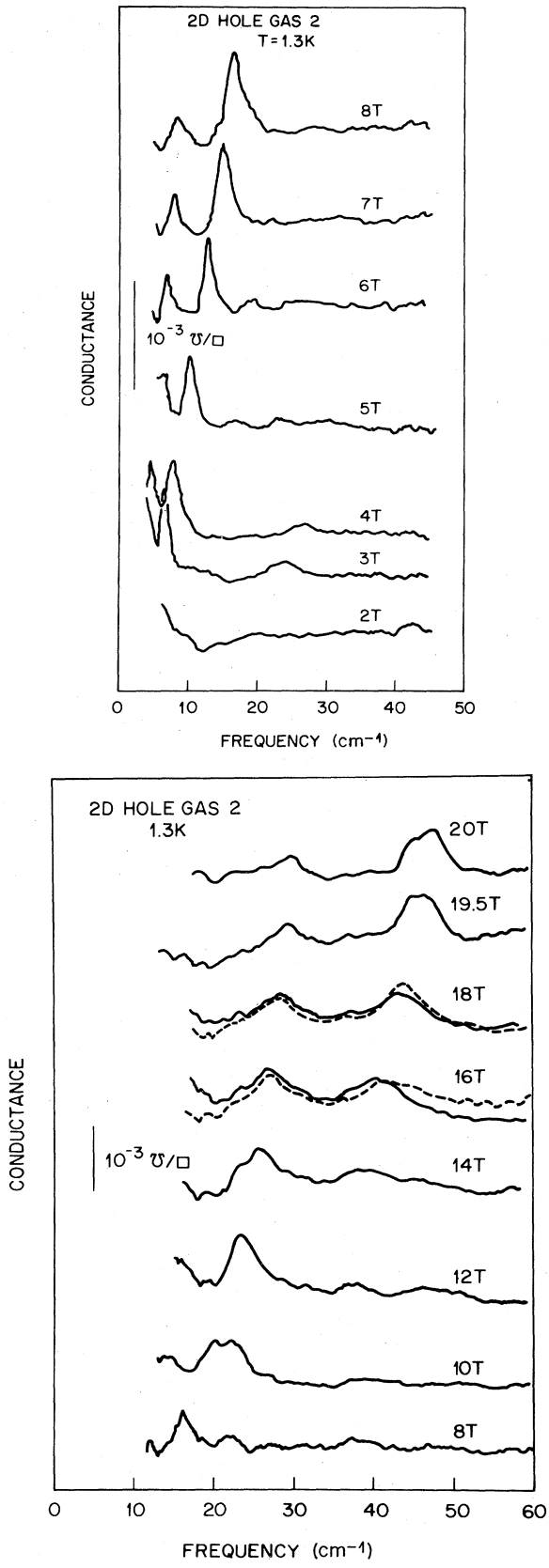

FIG. 4. Conductance versus frequency with magnetic field as a parameter at $\cong$1.3 K. Sample 2.

TABLE I. Electrical properties of samples at 4.2 K, where N_s is the hole density and p the mobility. Reference denotes wafer numbers.

Sample	N_s per layer (cm^{-2})	μ (cm^2/V sec)	Probable background doping	Reference
1	$\cong 5.0\times 10^{11}$	$\cong 7\times 10^3$	$n\cong 10^{15}$	WW II 7-8-82-1
2	$\cong 5.6\times 10^{11}$	$\cong 30\times 10^3$	$p\cong 10^{15}$	WW III 1-5-83-1
3	$\cong 4.6\times 10^{11}$	$\cong 40\times 10^3$	$n\cong 10^{15}$	WW II 5-20-83-2

ty determined from the periodicity in $1/B$ is 4.6×10^{11} cm^{-2}. A feature worth noting is that the minima which occur when the Fermi level lies between "spin"-split states at $N=3$ and $N=5$ are more pronounced than the minimum at $N=4$, which occurs when the Fermi level lies between Landau-split states. Here N indicates the number of completely filled Landau or spin levels. This is a direct indication that the spacing of the spin or Landau levels in this field range gives larger "spin" splitting than Landau-level splitting. It should be clear, however, that the orbital degeneracy of the holes makes the distinction between spin and orbital quantum numbers misleading.

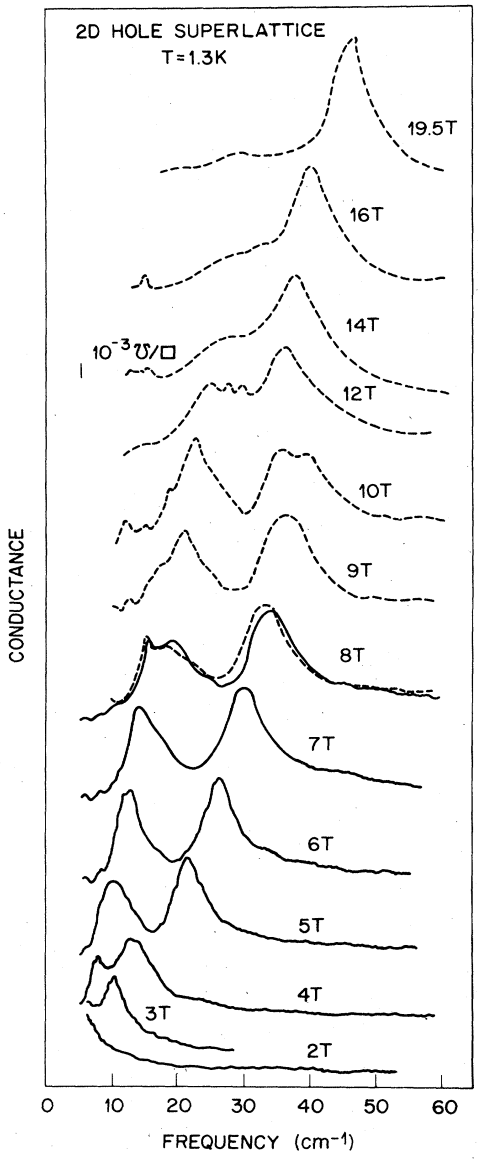

FIG. 5. Conductance versus frequency with magnetic field as a parameter at $\cong 1.3$ K. Sample 3.

CR's were observed by "sweeping" the frequency of far-infrared radiation transmitted through the sample with a Fourier-transform spectrometer while the sample was held at 1.3 K in magnetic fields from 0 to 20 T.[10] The experimental traces of conductance versus frequency for the three samples in question with magnetic field as a parameter are shown in Figs. 3—5. Although data are shown only for frequencies to 60 cm^{-1}, no other magnetic-field-dependent resonances were detected to 150 cm^{-1}.

In Figs. 6—8 the resonance positions versus magnetic field are plotted. The dominant or strong lines are indicated by the solid points.

DISCUSSION

Samples 2 and 3 are taken from the same wafers referred to as a triangular well and a square well by Eisenstein *et al.*[9] One is tempted to compare the cyclotron masses obtained from Figs. 7 and 8 with those obtained

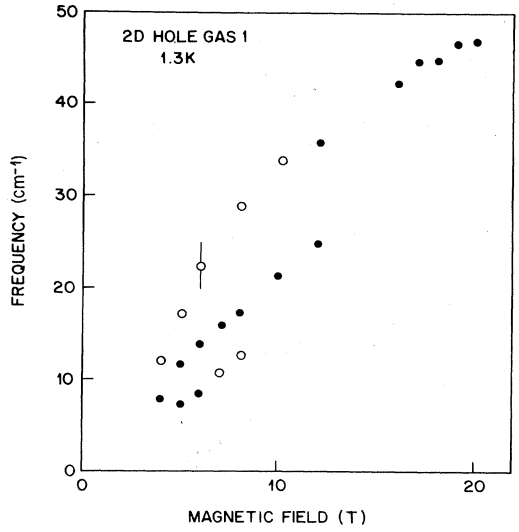

FIG. 6. Resonance frequencies of the strongest lines versus magnetic field. The strongest feature at a particular field is shown by a solid point. Sample 1.

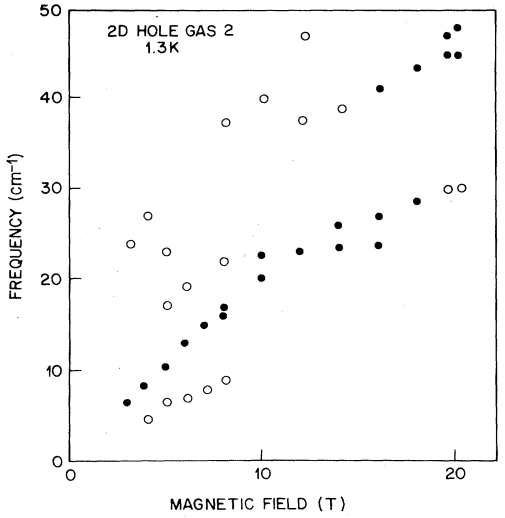

FIG. 7. Resonance frequencies of the strongest lines versus magnetic field. The strongest feature at a particular field is shown by a solid point. Sample 2.

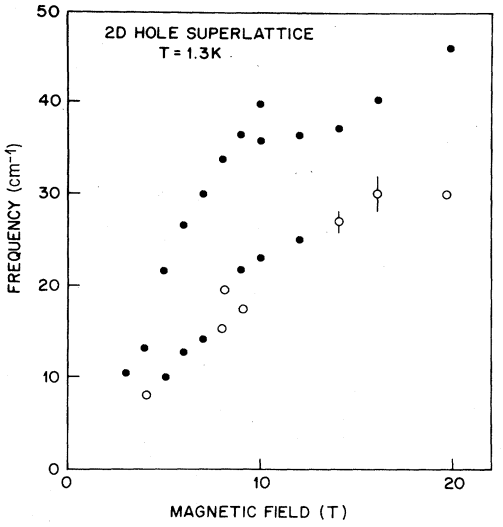

FIG. 8. Resonance frequencies of the strongest lines versus magnetic field. The strongest feature at a particular field is shown by a solid point. Sample 3. Superlattice.

from the temperature dependence of the Shubnikov–de Haas oscillations. However, the latter were obtained at substantially lower fields and it is clear from the experimental data that one cannot extrapolate to magnetic field values outside the data range with great confidence. Nonetheless, we make the comparison here. The superlattice sample reveals two masses in cyclotron resonance, $0.47m_0$ and $0.29m_0$, at a magnetic field of 4 T, whereas Eisenstein *et al.*[10] determine a single mass of $0.48m_0$ at 1.5 T. Sample 2, a triangular well, reveals two cyclotron masses, $0.47m_0$ and $0.8m_0$, at a field 4 T, as compared to Ref. 9, which determines a mass of $0.24m_0$ at 0.5 T and infers a second of $0.59m_0$. The agreement is not satisfactory but the magnetic field ranges in which the masses are determined are different.

To facilitate a discussion of these results, we describe a simple model calculation in which we simulate the confinement of the holes by taking a section through the 3D hole band structure at a wave vector k_z along the growth direction.[5,11,12]

The top of the valence band in GaAs is described by the following Hamiltonian[13,14]

$$H=\frac{\hbar^2}{2m}\left[\gamma_1(k_z^2+k_x^2+k_y^2)-2\gamma_2[k_x^2(J_x^2-\tfrac{1}{3}J^2)+k_y^2(J_y^2-\tfrac{1}{3}J^2)+k_z^2(J_z^2-\tfrac{1}{3}J^2)]\right.$$
$$\left.-\gamma_3[(J_xJ_y+J_yJ_x)(k_xk_y+k_yk_x)+(J_xJ_z+J_zJ_x)(k_xk_z+k_zk_x)+(J_yJ_z+J_zJ_y)(k_yk_z+k_zk_y)]+\frac{2e}{hc}kJ_zH_z\right]. \quad (1)$$

Here $\hbar$, m, and $\mathbf{k}$ are Planck's constants, the free-electron mass, and the hole wave vector, respectively. In a magnetic field normal to the plane of the 2D hole gas, the in-plane momentum is replaced by

$$\mathbf{k}=(1/i)\nabla+(e/hc)\mathbf{A}\ ,$$

where $\mathbf{A}$ is the vector potential. $\mathbf{J}$ is the angular momentum operator acting on the quartet of states at the top of the valence band. The material constants are taken from Skolnick[15] *et al.*,

$$\gamma_1=6.98,\ \gamma_2=2.25,\ \gamma_3=3.01\ ,$$

while k is scaled from Ge to 1.9 in GaAs. The q parameter found in Hensel and Suzuki[13,14] is set to zero for the sake of simplicity.

We simulate the hole confinement by introducing two parameters. Every term involved in k_z^2 in (1) is replaced by α^2, while every term linear in k_z, like k_zk_x, is replaced with βk_x. It has been argued that confinement has the effect of reducing the effectiveness of the latter terms.[5] ($\langle k_z\rangle=0$ and the linear terms must enter through higher-order perturbation). Although this is the simplest parametrization of the problem, we expect that Eq. (1) with α and β as adjustable parameters might provide a suitable phenomenology for describing the hole energy levels in a magnetic field. If the 2D hole gas lacks inversion symmetry, as it does for the single-interface samples, we may take β complex and find the spin degeneracy lifted for k_x or $k_y=0$. Since the warping is included in the

calculation ($\gamma_2 \neq \gamma_3$), we have an infinite matrix to diagonalize. We find, empirically, that limiting the matrix to the lowest 100 states is sufficient for calculation of the low-lying states at the Fermi level, provided that the magnetic field exceeds 3 T.

We fit the superlattice data as follows. Since we have quantum wells of the order of 100 Å wide, α is taken as $\pi/(100\ \text{Å})$. We adjust β to give a single strong line at approximately 45 cm^{-1} at 20 T: $\beta = \pi/(125\ \text{Å}^{-1})$. Without further adjustment we simply calculate the energy levels as a function of magnetic field, fill them according to Fermi statistics, and calculate the lines that should be observed in the experiment.

The results are shown in Fig. 9. The solid lines in the figure are the dominant transitions calculated with this model. Only rough semiquantitative agreement with experimental results is achieved. Similar comparisons can be made with the single-interface samples shown in Figs. 6 and 7 with the same degree of success.

The energy of the Landau levels versus magnetic field is shown in Fig. 10. The Fermi level is shown by the heavy line. We critically note that the strength of the Shubnikov–de Haas oscillations previously commented on in Fig. 2 should correlate with the discontinuity in the Fermi energy shown in Fig. 10. They do not.

It is also important to note that the model we have constructed here met with only limited success in the early stages of the studies of the 2D hole gas in Si MOSFET's.[5] There the calculated masses differed from the measured masses by nearly a factor of 2.

There are emerging more sophisticated calculations of the energy levels of the 2D hole gas in a magnetic field, and we compare the data for the superlattice with some of these calculations in Fig. 11.[3,4] These theories do not do better and the results at present have been given only for low magnetic fields. The results from Ekenberg and Altarelli[2] are not plotted. Broido *et al.*[3] argue that many-body interactions play a larger role in the 2D hole gas than for the 2D electron gas. Presumably, these effects must be included in a correct description of the cyclotron resonance of the 2D hole gas.

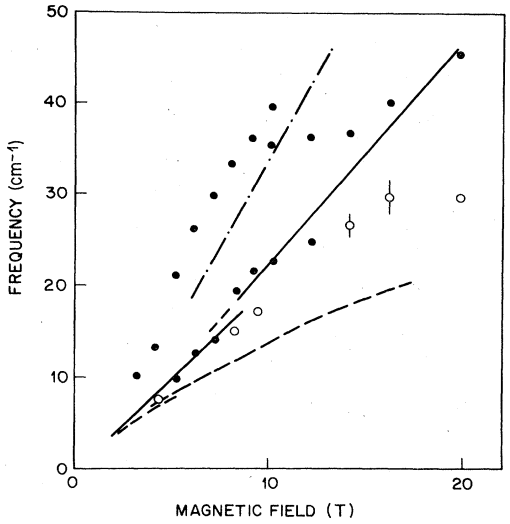

FIG. 9. Resonance frequencies of the strongest lines versus magnetic field. Points are obtained from Fig. 8, superlattice sample, while the solid and dashed lines are from the model calculation. The solid lines indicate the strongest line in the calculation.

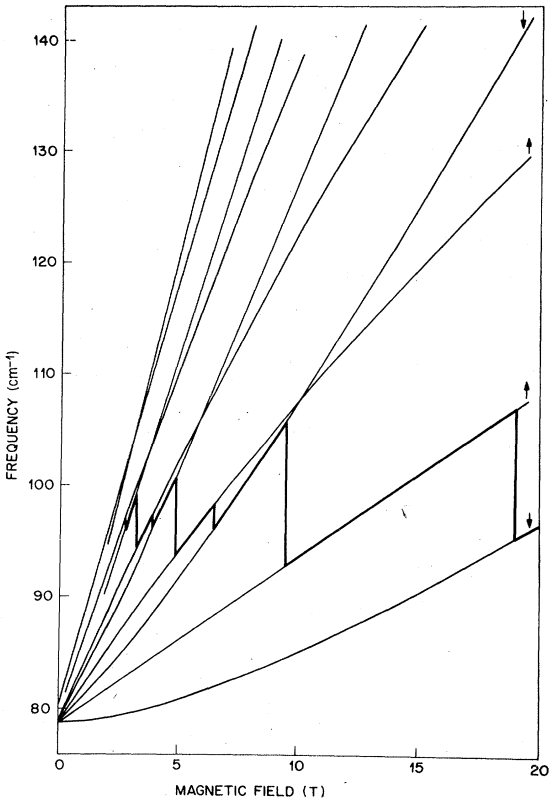

FIG. 10. Landau-level energy versus magnetic from the model described in the text. Note the alternation and crossing of the spin levels.

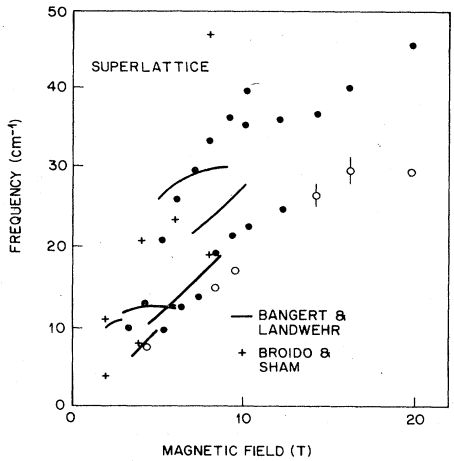

FIG. 11. Resonance frequencies of the strongest lines versus magnetic field. Points are obtained from Fig. 8, superlattice sample. The solid lines are from Bangert and Landwehr (Ref. 4). The crosses are from Broido and Sham (Ref. 3).

In summary, far-infrared cyclotron resonance of the 2D hole gas reveals a complex dependence on magnetic field that can be shown to be in rough semiquantitative agreement with the Landau-level splittings of a confined 2D hole gas. At present we do not understand the strength or multiplicity of the cyclotron resonance, especially at low or intermediate fields.

ACKNOWLEDGMENTS

It is a pleasure to acknowledge the support and technical assistance of L. Rubin and Bruce Brandt at the National Magnet Laboratory at the Massachusetts Institute of Technology, as well as valuable and interesting discussions with L. Sham and H. Stormer.

---

*Visiting scientist at the Francis Bitter National Magnet Laboratory, Massachusetts Institute of Technology, Cambridge, MA 02139.

[1]J. M. Luttinger, Phys. Rev. **102**, 1030 (1956).

[2]U. Ekenberg and M. Altarelli, Phys. Rev. B **30**, 3569 (1984).

[3]D. A. Broido and L. J. Sham, in *Proceedings of the 17th International Conference on the Physics of Semiconductors, San Francisco, 1984,* edited by J. D. Chadi and W. A. Harrison (Springer, New York, 1984), p. 337; Phys. Rev. B **31**, 888 (1984).

[4]E. Bangert and G. Landwehr, in Proceedings of the 1st International Conference on Superlattices, Microstructures and Microdevices, Champaign, Illinois, 1984 [Superlatt. Microstruc. **1**, 363 (1985)].

[5]For a review of work on *p*-channel MOSFET's, see T. Ando, A. B. Fowler, and F. Stern, Rev. Mod. Phys. **54**, 594 (1982).

[6]A. D. Wieck, E. Batke, D. Heitmann, and J. P. Kotthaus, Phys. Rev. B **30**, 4653 (1984).

[7]A. D. Wieck, E. Batke, D. Heitmann, J. P. Kotthaus, and E. Bangert, Phys. Rev. Lett. **53**, 493 (1984).

[8]H. L. Stormer, Z. Schlesinger, A. Chang, D. C. Tsui, A. C. Gossard, and W. Wiegmann, Phys. Rev. Lett. **51**, 126 (1983).

[9]J. P. Eisenstein, H. L. Stormer, V. Narayanamurti, A. C. Gossard, and W. Wiegmann, Phys. Rev. Lett. **53**, 2579 (1984).

[10]D. C. Tsui, S. J. Allen, Jr., R. A. Logan, A. Kamgar, and S. N. Coppersmith, Surf. Sci. **73**, 419 (1978).

[11]D. Coleman, R. T. Bate, and J. P. Mize, J. Appl. Phys. **39**, 1923 (1968).

[12]T. Sato, Y. Takeishi, and H. Hara, Jpn. J. Appl. Phys. **8**, 588 (1969).

[13]K. Suzuki and J. C. Hensel, Phys. Rev. B **9**, 4184 (1974).

[14]J. C. Hensel and K. Suzuki, Phys. Rev. B **9**, 4219 (1974).

[15]M. S. Skolnick, A. K. Jain, R. A. Stradling, J. Leontin, J. C. Ousset, and S. Askenazy, J. Phys. C **9**, 2809 (1976).